

2018

## Developmental stage influences chromosome segregation patterns and arrangement in the extremely polyploid, giant bacterium *Epulopiscium* sp. type B

Elizabeth Hutchison  
*SUNY Geneseo*, [hutchison@geneseo.edu](mailto:hutchison@geneseo.edu)

Follow this and additional works at: <https://knight scholar.geneseo.edu/biology>



Part of the [Bacteriology Commons](#)


---

### Recommended Citation

Hutchison, E., Yager, N. A., Taw, M. N., Taylor, M., Arroyo, F., Sannino, D. R., & Angert, E. R. (2018). Developmental stage influences chromosome segregation patterns and arrangement in the extremely polyploid, giant bacterium *Epulopiscium* sp. type B. *Molecular Microbiology*, 107(1), 68–80.

This Article is brought to you for free and open access by the By Department at KnightScholar. It has been accepted for inclusion in Biology Faculty/Staff Works by an authorized administrator of KnightScholar. For more information, please contact [KnightScholar@geneseo.edu](mailto:KnightScholar@geneseo.edu).

# Developmental stage influences chromosome segregation patterns and arrangement in the extremely polyploid, giant bacterium *Epulopiscium* sp. type B

Elizabeth Hutchison,<sup>1,2</sup> Nicholas A. Yager,<sup>1</sup>  
May N. Taw,<sup>2</sup> Matthew Taylor,<sup>1</sup> Francine Arroyo,<sup>2</sup>  
David R. Sannino<sup>2</sup> and Esther R. Angert <sup>2\*</sup>

<sup>1</sup>Department of Biology, SUNY Geneseo, Geneseo, NY, USA.

<sup>2</sup>Department of Microbiology, Cornell University, Ithaca, NY, USA.

## Summary

Few studies have described chromosomal dynamics in bacterial cells with more than two complete chromosome copies or described changes with respect to development in polyploid cells. We examined the arrangement of chromosomal loci in the very large, highly polyploid, uncultivated intestinal symbiont *Epulopiscium* sp. type B using fluorescent *in situ* hybridization. We found that in new offspring, chromosome replication origins (*oriCs*) are arranged in a three-dimensional array throughout the cytoplasm. As development progresses, most *oriCs* become peripherally located. Siblings within a mother cell have similar numbers of *oriCs*. When chromosome orientation was assessed *in situ* by labeling two chromosomal regions, no specific pattern was detected. The *Epulopiscium* genome codes for many of the conserved positional guide proteins used for chromosome segregation in bacteria. Based on this study, we present a model that conserved chromosomal maintenance proteins, combined with entropic demixing, provide the forces necessary for distributing *oriCs*. Without the positional regulation afforded by radial confinement, chromosomes are more randomly oriented in *Epulopiscium* than in most small rod-shaped cells. Furthermore, we suggest that the random orientation of individual chromosomes in large polyploid cells would not hamper reproductive success as it would in smaller cells with more limited genomic resources.

## Introduction

The bacterial chromosome is highly organized yet dynamic, as its position and conformation change throughout the cell cycle (Toro and Shapiro, 2010; Graumann, 2014; Le and Laub, 2014). Given that bacterial chromosomes are typically 1–10 Mb circular macromolecules, approximately 0.15–1.5 µm long, and housed in a volume generally 1–5 µm<sup>3</sup> (Young, 2006), a chromosome must be compacted >1000-fold to fit inside the cell (Holmes and Cozzarelli, 2000; Jun and Wright, 2010; Reyes-Lamothe *et al.*, 2012; Wang *et al.*, 2013). Bacteria regulate chromosome organization such that newly replicated chromosomes can be partitioned with high fidelity to daughter cells upon reproduction. The process has been studied in many model systems, including *Caulobacter crescentus* and *Escherichia coli* (Toro and Shapiro, 2010; Wang *et al.*, 2013). It also has been investigated during the development of specialized dormant cells such as endospores in *Bacillus subtilis* (Webb *et al.*, 1997), myxospores in *Myxococcus xanthus* (Tzeng and Singer, 2005) and spores in *Streptomyces* (Jakimowicz and van Wezel, 2012).

For many rod-shaped bacteria, chromosomes are organized longitudinally in the cell, with *oriC* (0°) and *ter* (180°) regions at opposite cell poles (or subpolar regions) (Mohl and Guber, 1997; Webb *et al.*, 1997; Jensen and Shapiro, 1999; Maloney *et al.*, 2009; Donovan *et al.*, 2010; Harms *et al.*, 2013; Vallet-Gely and Boccia, 2013; David *et al.*, 2014). Chromosome arrangement in a cell can vary during the life cycle of a bacterium, or change during different growth conditions (Wang and Rudner, 2014). In slow-growing *E. coli* cells, the *oriC* and *ter* regions are located primarily at the midcell, with the *ter* region more broadly distributed; with the left and right chromosome arms extending to either side, these chromosomes are in a transverse arrangement (Nielsen *et al.*, 2006; Wang *et al.*, 2006; Toro and Shapiro, 2010). Fast-growing *E. coli* adopt a more longitudinal orientation, emphasizing the adaptable nature of chromosome organization (Youngren *et al.*, 2014). Likewise, in *B. subtilis* cells, the orientation of chromosomes alternates between a longitudinal *ori-ter* pattern and a more

Accepted 6 October, 2017. \*For correspondence. E-mail era23@cornell.edu; Tel. (+1) 607 254 4778; Fax (+1) 607 255 3904.

transient transverse organization at different points in the cell cycle (Wang *et al.*, 2014).

A fine resolution study in *C. crescentus* examined 112 sites around the entire chromosome and found that the physical location of a chromosomal locus within the cell corresponded with its position on the chromosome (Viollier *et al.*, 2004). A similar relationship has been observed in *B. subtilis*, *E. coli* and *V. cholerae* (Teleman *et al.*, 1998; Niki *et al.*, 2000; Vallet-Gely and Boccard, 2013; David *et al.*, 2014). This pattern does not entirely hold true for *P. aeruginosa*, where the chromosome appears to be organized into large regions, centered around *oriC* and *dif*, and distant loci within one of these nearly megabase-sized domains often appear to colocalize (Vallet-Gely and Boccard, 2013).

Most of the work on chromosome organization has centered on bacteria that typically have one chromosome per cell (or two after replication), are approximately rod shaped and reproduce via binary fission. However, many bacteria have diverse cell and reproductive morphologies and harbor greater numbers of completely replicated chromosomes (Hansen, 1978; Minton, 1994; Jose Lopez-Sanchez *et al.*, 2008; Mendell *et al.*, 2008; Michelsen *et al.*, 2010; Ohtani *et al.*, 2010; Griese *et al.*, 2011; Pecoraro *et al.*, 2011; Angert, 2012). Previous work on chromosome organization of polyploid bacteria has focused on cyanobacteria. *Synechocystis* sp. PCC 6803 cells can contain tens to hundreds of chromosome copies (Griese *et al.*, 2011), and it has been reported that they do not always distribute DNA equally to daughter cells (Schneider *et al.*, 2007). A study using fluorescently tagged chromosomes revealed that *Synechococcus elongatus* PCC 7942 evenly spaces its 2–10 chromosome copies in a tandem array along the long axis of the cell (Jain *et al.*, 2012). Another study showed that while *S. elongatus* chromosomes were linearly organized in most cells, some cells had a random distribution (Chen *et al.*, 2012). With so few studies, there is still much to be revealed about how diverse species of polyploid bacteria organize their genomic resources, and whether or not they require novel mechanisms for chromosome organization.

The most extreme example of bacterial polyploidy known to date is *Epulopiscium* sp. type B, a member of the *Firmicutes* and an intestinal symbiont of an omnivorous surgeonfish, *Naso tonganus* (Clements *et al.*, 1989; Angert *et al.*, 1993). Although this bacterium cannot yet be grown in the laboratory, microscopy and genomic approaches have revealed substantial insight into its unusual cell and reproductive biology. During its life cycle, *Epulopiscium* sp. type B maintains its large size, with cigar-shaped cells ranging from approximately 100–300 µm in length (Angert and Clements, 2004). A large cell contains hundreds of picograms of DNA and results from quantitative PCR

indicate that *Epulopiscium* harbors tens of thousands of copies of its genome (Mendell *et al.*, 2008). Genome copy number scales with cell volume in *Epulopiscium* sp. type B and polyploidy appears to be key in allowing these giant cells to overcome diffusion-limited constraints on size. How these cells manage their genomic resources has not been characterized.

*Epulopiscium* sp. type B represents a diverse group of surgeonfish intestinal symbionts called 'epulos', which vary in size and reproductive mode (Clements *et al.*, 1989; Angert *et al.*, 1993). Some epulos only reproduce via production of internal offspring cells, others use multiple endospore formation, and some can undergo binary fission or a combination of binary fission and sporulation (Angert, 2005). Early stages of development of intracellular offspring in epulos are similar to forespore formation in *B. subtilis* (Miller *et al.*, 2011, 2012). While still contained in their mother cell, *Epulopiscium* sp. type B daughter cells begin a reproductive cycle by polar division and engulfment of polar offspring cells (granddaughter cells) (Fig. 1). After engulfment, the newest generation of offspring grows within their mother cell. Throughout development, DNA in *Epulopiscium* sp. type B exhibits stage-specific patterns of distribution (Angert and Clements, 2004).

Although epulos have not been cultured yet, these are attractive systems in which to address questions about chromosome organization in polyploid bacteria with diverse cellular morphologies. In this study, we used fluorescence *in situ* hybridization (FISH) to locate individual chromosomal loci within cells at difference stages of their developmental cycle and to begin to assess the organization of multiple chromosomes within large, highly polyploid

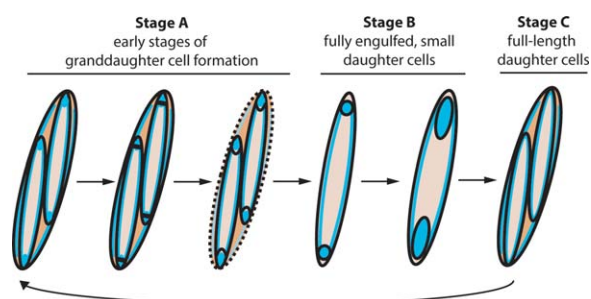


**Fig. 1.** The life cycle of *Epulopiscium* sp. type B. In this illustration, cell outlines are shown in black and DNA is shown in blue. In stage A, initiation of offspring cells begins while daughter cells are still contained within their mother cell. DNA accumulates at the poles of daughter cells. Daughter cells divide at extreme polar positions. These new offspring cells (granddaughter cells) are engulfed around the time the mother cell begins to deteriorate. The mother cell lyses, releasing the daughter cells. In stage B, fully engulfed offspring cells grow and elongate. In stage C, daughter cells have reached their size maximum and nearly fill the mother cell. DNA in these large daughter cells is located to the periphery of the cell. This cycle occurs over the course of 24 h and within an individual host, an *Epulopiscium* population is synchronized with respect to development.

bacteria. Our results suggest that *Epulopiscium* sp. type B manages an enormous number of chromosome copies using the foundational mechanisms employed by other bacteria. Some unusual cellular features, such as the formation of lateral offspring primordia, may require novel mechanisms as yet to be identified.

## Results

### *Epulopiscium* sp. type B DNA arrangement and *oriC* packing density change throughout development

*Epulopiscium* sp. type B cells exhibit dynamic changes in the localization of their DNA throughout development (Fig. 2). Of particular note are the unusual features that arise as offspring cells begin to form. Prior to polar

division, a portion of the mother-cell DNA condenses at the cell poles (Angert and Clements, 2004). The DNA of an offspring primordium organizes into string-like structures comprising a 'cap' of DNA that appears tethered to the pole (Fig. 2A and B) (Robinow and Angert, 1998). Polar division and engulfment of the polar cell traps this pole-associated DNA in an offspring cell (Figs 1, stage A, and 2C–F). In mother cells that produce more than two offspring, additional offspring form at lateral positions in the cell (Supporting Information Fig. S1).

We reasoned that the distribution of replication origins would also change throughout development in *Epulopiscium* sp. type B. A single chromosomal origin of replication was identified previously in the *Epulopiscium* sp. type B draft genome (Angert, 2012) and served as our initial target for FISH (see *Experimental procedures*; Fig. 3 and Supporting Information Table S1). We expect that for each individual chromosome in a cell, there will be a single fluorescent *oriC* focus. However, early in replication some origin regions will not be visually resolved and two *oriCs* may appear as a single focus. If DNA in *Epulopiscium* sp. type B is comprised solely of complete chromosome copies, no partial chromosomes or plasmids, we expect that thousands of resolved *oriC* foci will be seen in each large cell. We also expect *oriCs* to be most closely associated with one another in newly formed offspring, as DNA within these primordia and small cells appears to stain more brightly than other parts of the cell (see Fig. 2E, F and H–K). Intense DNA staining is often indicative of condensed chromosomes.

In mother cells with small offspring that are not yet fully engulfed, chromosomal *oriC* regions were primarily located at or near the periphery of the mother-cell cytoplasm (Fig. 3, stage A, and Supporting Information

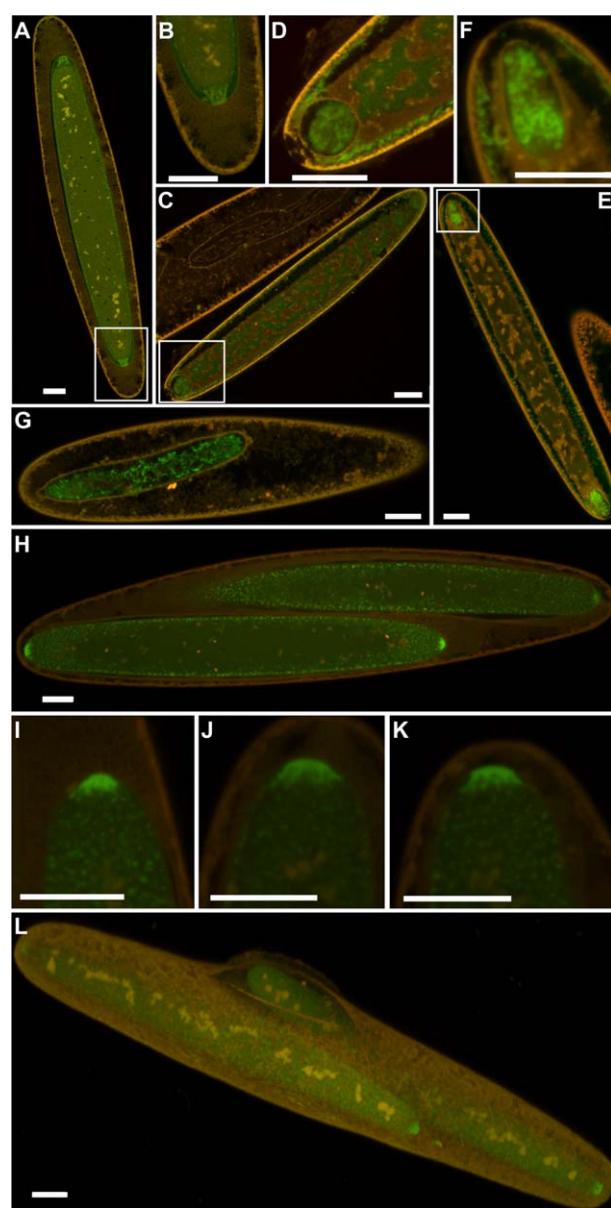


**Fig. 2.** DNA localization throughout *Epulopiscium* sp. type B development.

Confocal images of *Epulopiscium* cells stained with STYO9 (green, DNA) and Mitotracker Red FM (membrane); green autofluorescence in the membrane causes much of the membrane to appear yellow in these merged images. (A) Early in development, DNA accumulates at the poles of the mother cell and (B) often forms thread-like structures that appear tethered to the cell pole. (C) The mother cell engulfs the developing daughter cell completely, (D and F) leaving a void in the mother-cell DNA layer at each pole. (E) Engulfed daughter cells elongate, and (F) DNA is dispersed throughout the daughter cell. Panels (B), (D) and (F) show an enlargement of boxed regions in panels (A), (C) and (E), respectively. (G) As daughter cells elongate, DNA occupies most of the cytoplasmic volume but appears less compact than the DNA in smaller offspring cells. (H) Daughter cells continue to grow until they are almost the length of the mother cell. At late stages of development, daughter-cell DNA primarily occupies a layer beneath the cell membrane but also accumulates at the poles. Panels (I)–(K) show the polar regions of the daughter cells in panel (H) at a higher magnification. These are offspring (granddaughter cell) primordia. (L) 3D reconstruction showing a daughter cell emerging through a tear in the mother cell envelope. Scale bars indicate 10  $\mu$ m.



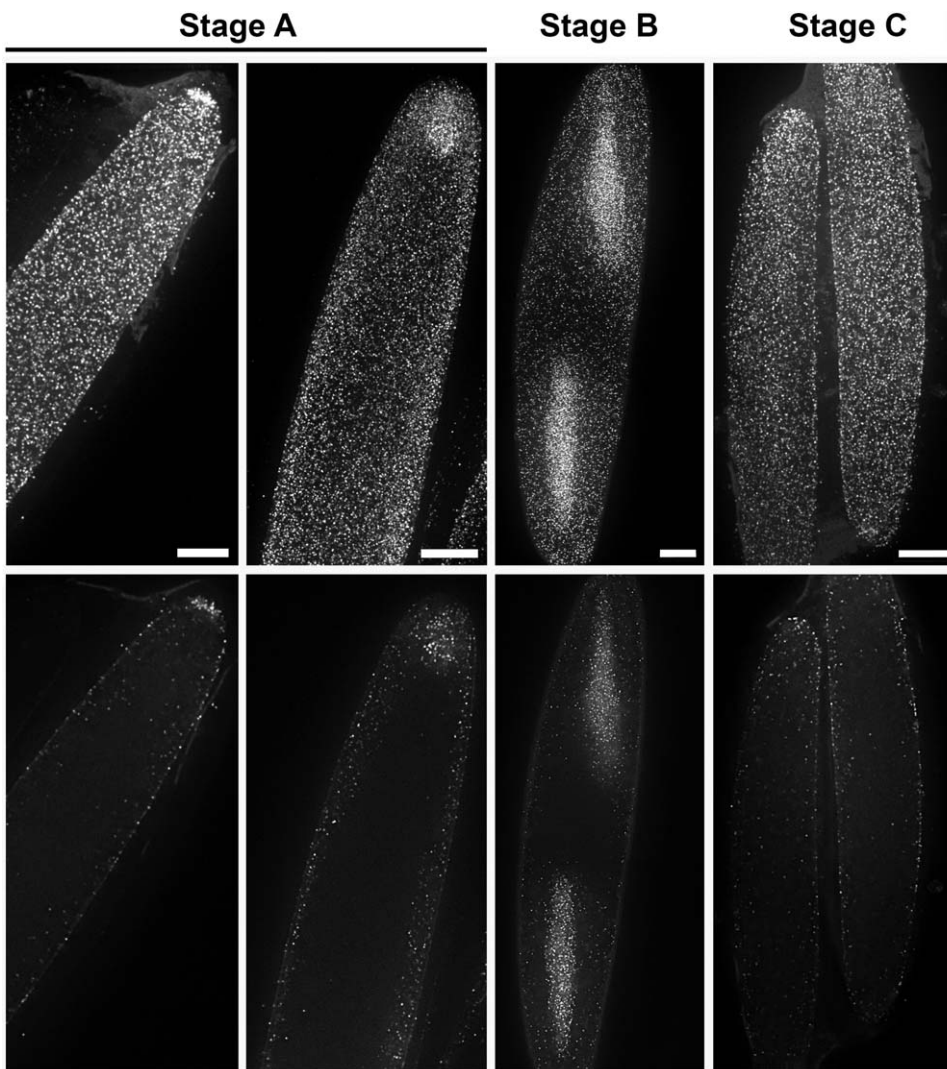


**Fig. 3.** Localization of the *Epulopiscium* sp. type B *oriCs* throughout development. The upper panels show composites of the complete z-stacks, and the bottom panels show a single plane from the middle of each of these z-stacks. For each life cycle stage, at least 35 cells were imaged, and cells pictured are representative of the dataset. Scale bars indicate 10  $\mu\text{m}$ .

Movie S1). Small patches of tightly clustered *oriC* foci were seen at the mother-cell poles early in offspring development. Likewise, clusters of origins were seen at lateral positions corresponding to locations where we observed lens-shaped offspring primordia (Supporting Information Fig. S1). In contrast, the *oriC* foci were located throughout the cytoplasm in small, fully engulfed offspring cells and offspring cells that had elongated (Fig. 3, stage B, and Supporting Information Movie S2). In offspring cells that had reached their full length, the mother cell was visible as only a faint outline surrounding these daughter cells, and fewer origin-region foci were observed in the mother cell than in the offspring cells (Fig. 3, stage C, and Supporting Information Movie S3). Most *oriC* foci were located at the periphery of the cytoplasm within large offspring cells although a few broadly spaced foci were seen deep within the offspring cytoplasm. This is consistent with previous observations (Ward *et al.*, 2009) that the amount of mother-cell DNA

(assessed via staining) diminishes at late stages of development. Overall, our results indicate that *Epulopiscium* sp. type B cells organize their *oriCs* in development-specific patterns that correspond to the location of DNA in the cell.

Using three-dimensional reconstructions, we plotted the location of replication origins and calculated the distance from each focus to all neighboring *oriC* foci. In stages A and C, the *oriCs* were primarily located at the cell periphery within large, nearly mature offspring cells or cells that were recently released from their mother cell (Supporting Information Fig. S2). The *oriCs* in stage B cells showed less of a bias toward the periphery. For all stages, we determined the average distance to the four nearest, visually distinct *oriC* foci (Fig. 4A–C, representing stages A–C, respectively). A summary of the distance distributions for cells from each stage are shown in Fig. 4D. The average distance between *oriCs* for stage A was 0.70  $\mu\text{m}$  (min = 0.11  $\mu\text{m}$ , max = 9.2  $\mu\text{m}$ , median = 0.66  $\mu\text{m}$ ), stage

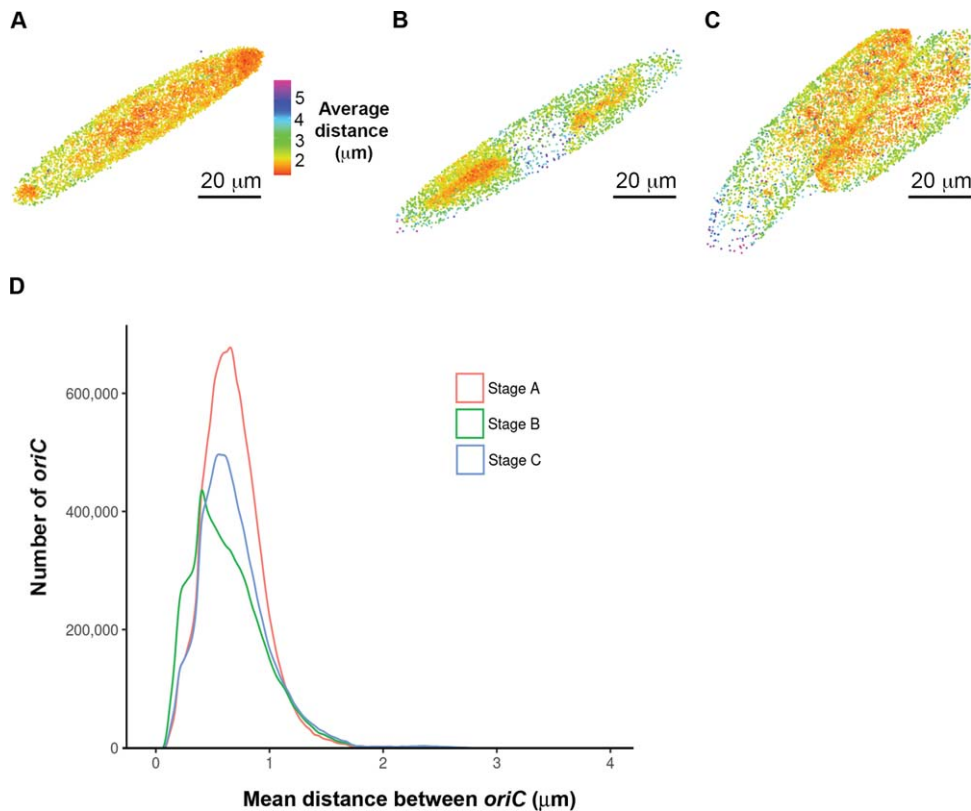


**Fig. 4.** Average distance between *oriC*s at different life cycle stages. FISH *oriC* foci are colorized to represent the average distance to the nearest 4 neighboring foci. Panels (A), (B) and (C) show single cells representing stages A, B and C, respectively. (D) Density estimation plots for *oriC* nearest neighbors for stage A ( $n = 26$ ), stage B ( $n = 37$ ) and stage C ( $n = 30$ ) cells. Distance distributions were significantly different between all stages using Kruskal–Wallis rank sum test ( $p < 2 \times 10^{-16}$ ), and a Dunn *post hoc* test (stage A vs. stage C,  $p < 0.05$ ; stage A vs. stage B,  $p < 1 \times 10^{-4}$ ; stage B vs. stage C,  $p < 1 \times 10^{-4}$ ).

B was  $0.67 \mu\text{m}$  (min =  $0.11 \mu\text{m}$ , max =  $8.5 \mu\text{m}$ , median =  $0.60 \mu\text{m}$ ) and stage C was  $0.73 \mu\text{m}$  (min =  $0.09 \mu\text{m}$ , max =  $9.8 \mu\text{m}$ , median =  $0.65 \mu\text{m}$ ). Though the distributions were significantly different between all three stages (Kruskal–Wallis rank sum test,  $p < 2.2 \times 10^{-16}$ ), the distributions for stages A and C were more similar to each other than each was to stage B ( $p < 0.05$  vs.  $p < 1 \times 10^{-4}$ ). Our data suggest that stage B cells with offspring that are fully engulfed and still small have a higher proportion of more closely spaced *oriC*s than stage A and C cells.

Next, we quantified the *oriC* packing density of *Epulopiscium* sp. type B cells throughout development. The z-stack for an individual cell was analyzed using an algorithm we developed for removing background fluorescence and counting *oriC* foci (see *Experimental procedures*). Our program identified the cell periphery and we used these coordinates to calculate the cell volume. For these measures, foci in the mother cell and offspring were counted. The number of *oriC* foci in a cell was used as a proxy for chromosome number. On average, *Epulopiscium* sp. type B cells had  $0.10$  *oriC* per  $\mu\text{m}^3$ . Stages A, B and C cells had median densities of  $0.1114$ ,  $0.0844$  and  $0.0663$  *oriC* per  $\mu\text{m}^3$ , respectively (Fig. 5A). A Kruskal–Wallis rank sum test indicated a statistically significant difference in the three distributions ( $\chi^2 = 31.477$ ,  $n = 82$ ,  $df = 2$ ,  $p\text{-value} < 1 \times 10^{-7}$ ),

and a Nemenyi pairwise comparison test found that the *oriC* packing density in stage C was significantly different from both stage A and stage B cells (also see Fig. 5B). These results indicate that *oriC*-per- $\mu\text{m}^3$  packing density is slightly higher in the earlier stages of offspring development and decreases once daughter cells begin to elongate.

The number of *oriC* foci per cell increased linearly with cell size (Fig. 5B) and ranged from 597 to 9436 per cell. There was cell-to-cell variability, resulting in a fairly broad range for each stage. The lower *oriC* packing density in stage C may be a consequence of the observed decrease in mother-cell DNA as offspring cells mature (Ward *et al.*, 2009). This may explain why many of the stage C cells lie below the regression line in Fig. 5B. The previous study by Mendell *et al.* (2008) assessed *Epulopiscium* sp. type B ploidy using quantitative PCR and found an average of  $0.53$  chromosome copies per  $\mu\text{m}^3$ . This value is approximately fivefold higher than our estimates. Control experiments using our FISH protocol to detect chromosomes in sporulating *B. subtilis* showed that an average of 78% of cells (in replicate tests) had both *oriC* and *ter* probes successfully hybridize, and of the cells labeled with both probes  $\sim 85\%$  had *oriC* localized at the cell pole (Supporting Information Fig. S3). Despite the lower

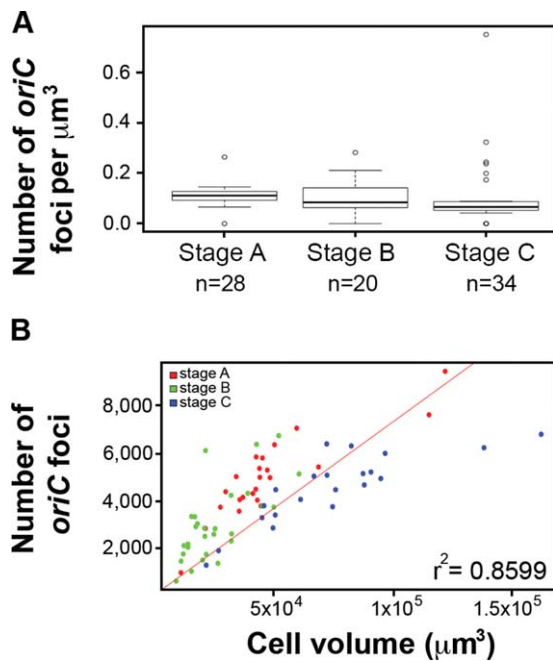


**Fig. 5.** Quantification of *oriC* packing density in *Epulopiscium* sp. type B mother and daughter cells.

A. Box plots show variation in *oriC* packing density between different life cycle stages in *Epulopiscium* sp. type B. Cells in stages A, B and C were taken from 2, 3 and 5 independent fish samples, respectively. A Kruskal–Wallis rank sum test identified a significant difference between stages A, B and C ( $p < 1 \times 10^{-7}$ ), and a Nemenyi pairwise comparison showed that stage C cells were significantly different than both stage A ( $p < 0.05$ ) and stage B ( $p < 0.05$ ) cells, while there was no significant difference between stage A and B cells ( $p = 0.97$ ).

B. The linear correlation between cell size and *oriC* number.

numbers recovered using FISH, we found that our FISH protocol provided a good and consistent estimate of the relative positions and numbers of resolved chromosome replication origins *in situ*.

We next quantified the number and packing density of *oriCs* in sibling cells (Fig. 6). We reasoned that if the number of chromosomes partitioned to each offspring cell is similar, then sibling *oriC* numbers should be comparable. Stage B offspring were ideal for this analysis since they are relatively small but fully engulfed, and their *oriC* foci can be easily distinguished from those of the mother cell. At this stage of development, the *oriC* packing density in offspring cells is slightly higher, though not significantly different, from their corresponding mother cell (Fig. 6A; Kruskal–Wallis,  $\chi^2 = 7$ ,  $df = 7$ ,  $p = 0.43$ ). Though some variation was observed between sibling *oriC* counts, seven of the eight sibling pairs analyzed had *oriC* counts that were within one doubling (Fig. 6B). Only one pair differed by more than twofold (with 261 and 588 *oriCs*). These results suggest that each offspring cell receives about the same number of chromosomes.

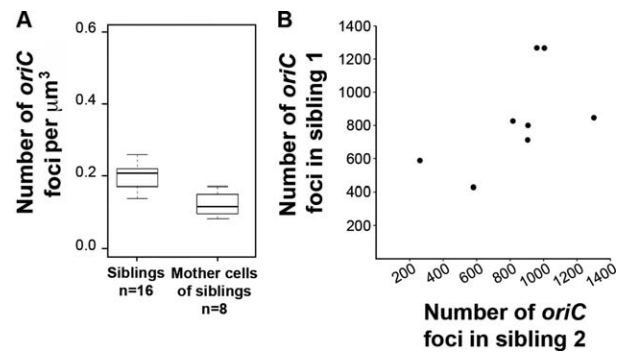


**Fig. 6.** Density and *oriC* counts in offspring and siblings from Stage B cells.

A. Boxplot shows *oriC* density in offspring cells early in development and the packing density of their corresponding stage B mother cells (no significant difference between offspring and mother cells; Kruskal–Wallis,  $\chi^2 = 7$ ,  $df = 7$ ,  $p = 0.43$ ).

B. Total *oriCs* in sibling cells from A. Each point represents the *oriC* counts from two siblings within the same mother cell.

#### Chromosome orientation appears less constrained in *Epulopiscium* sp. type B compared to other bacterial models

Previous studies in model systems have shown that the *oriC* and *ter* regions typically maintain a specific orientation in the cell. To explore chromosome alignment in *Epulopiscium* sp. type B, we simultaneously labeled two different chromosome regions, each with a different fluorophore. We could not bioinformatically detect a terminus region in the *Epulopiscium* sp. type B draft genome, and thus, we could not evaluate chromosome orientation using *oriC* and *ter* as has been done in other bacteria. Previous work in *C. crescentus* showed that chromosome regions 125–250 kb apart occupied distinct yet adjacent regions in the cell (Viollier *et al.*, 2004). Using *Epulopiscium* probes > 100 kb apart, it was difficult to draw any conclusions about chromosome orientation because there was little to no overlap between fluorescent foci and it was impossible to know which two foci represented sites on a single chromosome. Unlike polyploid cyanobacteria (Jain *et al.*, 2012), intrachromosomal distances were not less than interchromosomal distances in *Epulopiscium*. Through further refinement, we found that placing the probes closer together (65–80 kb; Supporting Information Table S1) produced resolved fluorescent foci with some remaining overlap between the two different foci. Even in these dual-labeled cells we were unable to discern any bias in chromosome orientation (Fig. 7). Likewise, we were unable to detect a bias in orientation of the two probes in offspring primordia (Fig. 7B).

We performed FISH studies on smaller epulo morphotypes as well to see if chromosome orientation could be resolved in cells with fewer chromosomes (Supporting



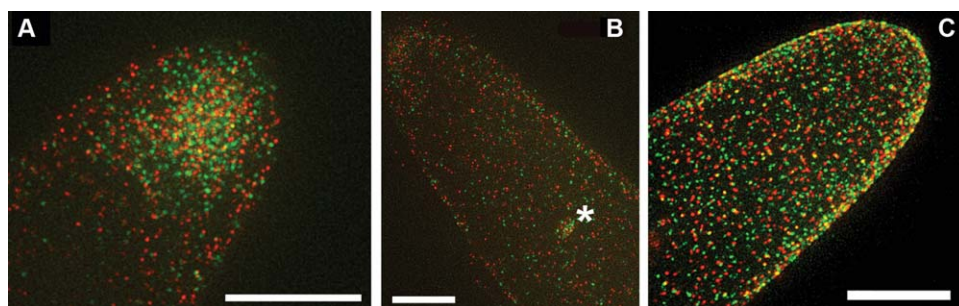


**Fig. 7.** Localization of two different chromosomal regions to assess chromosome orientation in *Epulopiscium* sp. type B. *Epulopiscium* sp. type B cells were hybridized with probes for two chromosomal regions (approximately 65 kb apart), labeled with either a green or red fluorescent probe. Images shown in the three panels are composites of the complete z-stack through the cell. (A) Stage A cell, (B) cell with a lateral offspring (indicated by asterisk) and (C) stage C cell. Scale bars represent 10  $\mu$ m.

Information Figs S4 and S5). We were however unable to detect any pattern of chromosome alignment relative to cell poles or other structures. From these images we concluded that these smaller epulos are also highly polyploid and none of these cells appear to maintain a specific orientation of their chromosomes that would be evident by FISH.

*The Epulopiscium sp. type B genome contains homologs to most of the known chromosome organization, maintenance and repair genes*

To assess whether *Epulopiscium* sp. type B has the genetic potential to organize and maintain chromosomes in a similar manner to well-characterized bacterial model systems, we searched the *Epulopiscium* sp. type B draft genome (Miller *et al.*, 2012) for homologs of *B. subtilis* genes involved in chromosome organization, partitioning and repair (see *Experimental procedures*). The complete genome of *Cellulosilyticum lentocellum*, an endospore forming relative of *Epulopiscium* sp. type B, was searched as well. Since *B. subtilis* (class Bacilli) and *Epulopiscium* (class Clostridia, family Lachnospiraceae) are distant relatives within the Firmicutes, a comparison with *C. lentocellum* (family Lachnospiraceae) provided a meter for conserved genes that may be difficult to identify using BLAST. We used a method similar to Miller *et al.* (2012), combining reciprocal best blast hits and synteny to predict homologs in the *Epulopiscium* sp. type B genome. Results from the genome comparison are shown in Supporting Information Table S2. Overall, genes involved in chromosome partitioning, condensation and organization (such as *divIVA*, *soj*, *spo0J* and *smc*) are conserved between *B. subtilis*, *C. lentocellum* and *Epulopiscium* sp. type B. In both *Epulopiscium* sp. type B and *C. lentocellum*, we were unable to find homologs of *racA*, *recJ*, *recX*, *minJ*, *comN*, several primosome components, non-homologous end-joining repair components, the helicase *recQ*, and several

lesion-bypass polymerases. *Epulopiscium* sp. type B was missing genes that were present in *C. lentocellum*, such as *lexA*, *recN*, *recS*, possibly *recU*, several *apurinic/apyrimidinic* (AP) endonucleases and AP lyases and *ripX*. Though some categories of repair genes are not accounted for in the *Epulopiscium* sp. type B genome, conserved chromosome organization genes are present. Genome data indicate that *Epulopiscium* sp. type B is likely using a similar genetic toolset as other characterized bacteria to organize its chromosomes. This preliminary survey indicates differences between chromosome resolution and repair practices in *Epulopiscium* sp. type B compared to typical endospore-forming bacteria.

## Discussion

*Epulopiscium* sp. type B and related intestinal symbionts provide unique systems for studying the organization of chromosomes in highly polyploid bacteria with diverse cell morphologies. We found that *oriC* spacing in *Epulopiscium* sp. type B cells is consistent within populations of cells at a particular stage of development, and the average distance between neighboring *oriCs* changes throughout development. As an offspring cell grows, *oriCs* become less tightly packed and they are redeployed to the outer edges of the cytoplasm. In contrast, the rod-shaped polyploid cyanobacterium *S. elongatus* contains evenly spaced chromosome replication origins, arranged in a line spanning the long axis of the cell (Jain *et al.*, 2012). Like *Epulopiscium*, these cyanobacteria exhibit a complex internal structure that includes thylakoid membranes and intracellular inclusions. It has been suggested that intracellular structures (i.e., carboxysomes) contribute to the organization of chromosomes in these cells (Jain *et al.*, 2012). We suspect that the linear arrangement of chromosomes in *S. elongatus* may be enforced by radial confinement that appears to dictate the intracellular positioning of loci in model systems



(e.g., *E. coli*, *C. crescentus* and *B. subtilis*) (Jun and Mulder, 2006).

We were surprised to find changes in *oriC* spacing in *Epulopiscium* sp. type B cells throughout development. Differences in average interchromosomal distance are not simply due to an increase in cell size and the dispersal of a finite number of chromosomes. In a previous study, sites of replication were labeled in living *Epulopiscium* sp. type B cells with incorporation of the nucleotide analog bromodeoxyuridine (BrdU) (Ward *et al.*, 2009). As expected, BrdU labeled the DNA within growing offspring cells, but we found that mother-cell DNA was labeled as well, even at late stages in development, such as stage B in Figs 1 and 2. This observation suggests that 'somatic' chromosomes in the mother cell continue to replicate and total chromosome number increases as the mother cell and its internal offspring expand. It is possible that replication may not keep pace with cell growth. We suggest another interpretation; that increases in distance between chromosomes may be a function of shifting toward more transcriptionally active chromosomes. Previous studies have shown that transcription rates can influence chromosome structure and compaction (Cagliero *et al.*, 2013; Le *et al.*, 2013; Marbouty *et al.*, 2015; Le and Laub, 2016). We speculate that when a type B cell is first formed, it is packed full of multiple copies of its genome which do not become transcriptionally active until later stages of growth. The lowest packing density of *oriCs* in stage C cells may be due to the elimination of mother cell chromosomes, corresponding with diminution of DNA staining in mother cells just prior to offspring release (Ward *et al.*, 2009).

In this and a previous study (Mendell *et al.*, 2008) we noted that *Epulopiscium* sp. type B cells have fewer chromosomes per cubic micron of cytoplasm than *B. subtilis*. For these estimates we factored in total cytoplasmic volume. Using FISH to locate individual *oriCs* *in situ* we now are able to take a more refined look at the spacing of chromosomes in these cells and find that the average distance between *oriC* foci in *Epulopiscium* type B cells ( $<1\mu\text{m}$ ) is smaller than the distance between resolved *oriCs* in *B. subtilis*. This suggests that the peripheral cytoplasm in *Epulopiscium* is similar in its DNA content and chromosome packing density to a smaller bacterium. Moreover, the peripheral location of *oriC* foci in *Epulopiscium* may indicate a functional similarity to *Thiomargarita namibiensis*. This giant sulfur-oxidizing bacterium contains a large, nitrate storage vacuole which takes up as much as 98% of the cell volume. This membrane-bound compartment confines the active cytoplasm and nucleoids to a thin layer just beneath the cell surface (Schulz *et al.*, 1999). Maintaining chromosomes at the periphery of the cytoplasm may

be an important paradigm for large bacterial cells with a low surface-to-volume ratio.

We did not observe a pattern for chromosome orientation in any *Epulopiscium* cells. It is possible that the complexity of the intracellular membrane system in the larger cells confounded this analysis (Robinow and Angert, 1998). We hypothesize that in these highly polyploid cells, physical position of chromosomes relative to cell poles is not as critical for chromosome function or segregation as it is for cells with smaller volumes and more limited genetic resources that must be completely partitioned to offspring cells for division to occur.

Our observations of *Epulopiscium* sp. type B chromosome segregation and orientation do not exclude a model based on entropic demixing (Jun and Mulder, 2006; Jun and Wright, 2010). In addition, the genome of *Epulopiscium* sp. type B codes for numerous predicted membrane-bound and secreted proteins (Miller *et al.*, 2012). It is possible that transertional forces (Roggiani and Goulian, 2015) influence the peripheral location of transcriptionally active chromosomes in large offspring and mother cells.

Chromosome location and position in bacteria is achieved in part by proteins that function as markers of the cell pole (Laloux and Jacobs-Wagner, 2014) and work in concert with DNA-bound proteins and physical forces that help segregate chromosomes. DivIVA in *B. subtilis* forms oligomers that can recognize the negative (concave) curvature of the membrane at the cell poles (Lenarcic *et al.*, 2009; Ramamurthi and Losick, 2009; Ramamurthi, 2010). Dynamic membrane curvature sensing could be important for *Epulopiscium* sp. type B, as it forms new polar offspring cells and the type B genome has a *divIVA* ortholog along with *parAB* orthologs *soj* and *spo0J*. However, initiation of offspring at locations other than the cell pole (e.g., see Supporting Information Fig. S1) may not have a clear positional cue. The infolded cell membrane at locations away from the poles creates a surface with a mix of concave and convex curvatures, so it remains unclear what dictates the sites where lateral offspring primordia arise. Additional factors that influence subcellular organization and protein localization in bacteria include: differences in membrane lipid composition, nucleoid occlusion, cell division site location, changes in membrane potential or fluidity and movement of peptidoglycan synthesis machinery (Govindarajan *et al.*, 2012; Laloux and Jacobs-Wagner, 2014). It does not seem that nucleoid occlusion is important in large *Epulopiscium* cells as rings of FtsZ form over densely packed polar DNA (Angert and Clements, 2004). Almost nothing is known about the composition of membrane lipids, peptidoglycan structure or membrane potential in *Epulopiscium*

spp., yet these present intriguing possibilities as contributors to cellular organization.

Our analyses suggest that *Epulopiscium* sp. type B has retained the same highly conserved genes required for chromosome maintenance and segregation as other bacteria. We hypothesize that these guides combined with entropic demixing of chromosome copies and perhaps transertion could provide the necessary forces to distribute chromosomes in these giant polyploids. Without the positional regulation afforded by radial confinement, chromosomal loci may be more randomly oriented in *Epulopiscium* than in most small rod-shaped cells. This could compromise the efficient segregation of complete chromosomes into offspring cells but this potential liability is overcome by the sequestration of multiple chromosomal copies in an offspring cell. Most of the sibling pairs contained *oriC* counts that were within one doubling of one another. This suggests that *Epulopiscium* sp. type B chromosome partitioning into offspring is not an entirely random process and that division site selection may dictate the number of chromosomes inherited.

Given the current data, we speculate the following model where different forces direct the position and spacing of chromosomes in these cells. First, as offspring primordia form, proteins associated with tethering replication origins to the cell pole and DNA condensation are of primary importance. After offspring cells are engulfed, entropic demixing helps separate and segregate chromosomes in a three-dimensional array. Chromosomes are transcriptionally inactive and condensation proteins likely assist in chromosome separation. As the offspring enlarge, chromosomes within offspring and mother cells replicate to support the metabolic activity of growing cells. Transcription of membrane proteins begins in offspring and transertion may help enforce the peripheral location of chromosomes. Dismantling chromosomes in the mother cell precedes mother-cell death and offspring release. This model provides a foundation for future studies of chromosome dynamics in large polyploid bacteria and for understanding how previously described chromosome organization forces might function in a non-model system.

## Experimental procedures

### Sample collection

*Naso tonganus* and *Naso lituratus* were caught by spear off the coast of Lizard Island, Australia in 2005 and 2011 and in the Sampan Channel, Oahu, HI, in April 2012, respectively. Intestinal contents were fixed in 80% ethanol and stored at  $-20^{\circ}\text{C}$ . To isolate individual cells for DNA extraction or for FISH analysis, cells were handpicked and

sequentially transferred five times through buffered ethanol [80% ethanol, 50 mM Tris-HCl (pH 8.0)] using a standard pipettor and a dissecting microscope (Nikon SMZ-U).

### DNA extraction

For *Epulopiscium* sp. type B cells, approximately 5000 cells were picked and washed five times in buffered ethanol. Cells were pelleted by centrifugation for  $< 1$  min at  $13,000g$  and the pellet was washed twice with 10 mM Tris-HCl (pH 8.0). The bacterial pellet was resuspended in 300  $\mu\text{l}$  of TE/SDS buffer (10 mM Tris pH 8.0, 5 mM EDTA, 0.5% SDS) plus 3  $\mu\text{l}$  of a 25 mg proteinase K  $\text{ml}^{-1}$  stock solution (Sigma-Aldrich, MO) and incubated at  $50^{\circ}\text{C}$  for 45 min. The lysate was extracted once with phenol:chloroform:isoamyl alcohol (25:24:1), and DNA precipitated from the aqueous phase with 0.3 M sodium acetate and 2 volumes of 100% ethanol. The DNA pellet was washed twice with cold 70% ethanol, dried and treated with RNase A (10  $\mu\text{g ml}^{-1}$  in 10 mM Tris, pH 8.0) for 30 min at  $37^{\circ}\text{C}$ .

### FISH probe synthesis

Probes for fluorescence *in situ* hybridization were constructed by amplifying 4–5 small DNA segments designed to cover one larger, contiguous 10–12 kb region of genome. Primers used are listed in Supporting Information Table S1. PCR was performed using Qiagen HotStarTaq Master Mix, per manufacturer's recommendations. Probes were labeled with tetramethyl-rhodamine-5-dUTP (cat. no. 11534378910; Roche, Germany) or Green 500 dUTP (cat. no. ENZ-42845; Enzo Life Sciences, Inc., NY) using a nick translation mix (cat. no. 11745808910; Roche, Germany). Nick translation was allowed to proceed for 130 min at  $15^{\circ}\text{C}$  and stopped with 1  $\mu\text{l}$  of 0.5 M EDTA by incubating at  $65^{\circ}\text{C}$  for 15 min. Probes were precipitated with sodium acetate and ethanol, resuspended in water and stored at  $-20^{\circ}\text{C}$ .

### Fluorescence in situ hybridization

FISH was carried out based on a fusion of two protocols, one for bacterial FISH (Jensen and Shapiro, 1999) and one for embedding cells in acrylamide pads for imaging and FISH analysis (Bass *et al.*, 1997). Several thousand *Epulopiscium* sp. type B cells were handpicked and washed five times in ethanol wash buffer. Cells were placed into a microcentrifuge tube coated with 1% (wt/vol) BSA (the BSA coating ensures that cells will pellet once buffers are added; ethanol-fixed cells do not pellet well in tubes without a BSA coating). Cell suspensions were centrifuged for a few seconds at  $13,000g$  and washed three times with 1 ml of Buffer A (15 mM PIPES-NaOH, pH 6.8, 80 mM KCl, 20 mM NaCl, 0.5 mM EGTA, 2 mM EDTA, 0.15 mM spermine tetrahydrochloride, 0.05 mM spermidine and 0.32 M sorbitol) (Bass *et al.*, 1997). After the final wash, cells were resuspended in approximately 50  $\mu\text{l}$  of Buffer A. A total of 5  $\mu\text{l}$  of this cell suspension was placed onto a 22 mm  $\times$  22 mm coverslip coated in 0.1% (vol/vol) poly-L-lysine (cat. no. P8920; Sigma-Aldrich, MO.). Next, a polyacrylamide mixture (50  $\mu\text{l}$

Buffer A, 50  $\mu$ l 30% vol/vol bis-acrylamide, 5  $\mu$ l of a 10% wt/vol sodium sulfite solution and 5  $\mu$ l of a 10% wt/vol APS solution) was made, quickly mixed and 5  $\mu$ l was placed on top of the cell suspension on the coverslip. A regular (non-coated) coverslip was placed on top of the cell suspension/acrylamide mix and left to polymerize at room temperature for 1 h. This coverslip sandwich was very carefully opened using a razor blade. The bottom coverslip, with the thin acrylamide pad still attached, was placed pad side up into a small petri dish.

Acrylamide pads were washed briefly (1–2 min) in 500  $\mu$ l of 30 mM phosphate buffer, pH 7.5. Excess buffer was removed by aspiration. Next, pads were fixed in 500  $\mu$ l of 2.5% (vol/vol) formaldehyde in 30 mM phosphate buffer for 15 min at room temperature, followed by 45 min on ice. Pads were washed three times in Buffer A (2–5 min each wash) and incubated in 500  $\mu$ l of 2 mg proteinase K  $\text{ml}^{-1}$  in buffer A for 1–3 min at 50°C. Pads were immediately washed three times with 2 $\times$  SSCT (300 mM sodium chloride, 30 mM sodium citrate, 0.1% vol/vol Tween-20, pH 7.0). Pads were washed an additional three times with 2 $\times$  SSCT, for 5 min each. Pads were incubated in 2 $\times$  SSCT/50% (vol/vol) formamide for 30–60 min at 37°C. Next, coverslips were placed (pad side up) onto a clean, labeled microscope slide. Approximately 100–200 ng of probe was mixed with hybridization buffer (3 $\times$  SSC/50% vol/vol formamide/10% wt/vol dextran sulfate) to a final volume of 50  $\mu$ l and pipetted onto the acrylamide pad. A new coverslip was placed on top of the pad, and a seal of rubber cement was placed at the edges of the coverslip to prevent the pad from drying out. The slide was incubated at 37°C for 30 min to allow probe to saturate the pad. Slides were then heated at 96°C for 6 min on a heat block and hybridized overnight (14–18 h) at 42°C. From this point on, pads were protected from light as much as possible. First, the rubber cement and top coverslip were removed, and the coverslip with the acrylamide pad was placed into a new petri plate. The pad was washed two times in 2 $\times$  SSCT/50% (vol/vol) formamide for 30 min at 37°C, once in 2 $\times$  SSCT/25% (vol/vol) formamide for 10 min at room temperature and three times in 2 $\times$  SSCT for 10 min at room temperature. The pads were washed briefly with Buffer A. Each pad was stained with 500  $\mu$ l of 2  $\mu$ g DAPI  $\text{ml}^{-1}$  in Buffer A for 30 min at room temperature. Excess DAPI was rinsed out by washing the pad three times with Buffer A for 10 min. Pads were then coated generously with the antifade reagent DABCO (2.5% wt/vol DABCO [1,4 diazabicyclo-(2,2,2) octane, Sigma D-2522], 50 mM Tris pH 8.0, 90% vol/vol glycerol). New coverslips were placed on top of the pads, and any excess DABCO was aspirated off. Slides were sealed with two coats of nail polish and stored at –20°C.

### Microscopy

Confocal images were taken on a Zeiss LSM710 laser scanning microscope at the Cornell Biotechnology Resource Center. All FISH pictures were taken on a Deltavision Spectris DV4 deconvolution microscope (Applied Precision Instruments, PA). For single probe experiments, images were taken 0.5  $\mu$ m apart with an

exposure of 0.5 s for rhodamine probes through the complete depth of the sample, with a 60 $\times$  Olympus lens (N.A. 1.4). For dual probe experiments, sections were taken 0.3  $\mu$ m apart, with an exposure time of 0.5 s for rhodamine and 0.75–1.0 s for rhodamine green through the complete thickness of the sample, with a 100 $\times$  Olympus lens (N.A. 1.4). The 3D stack of images was deconvolved using a constrained iterative deconvolution algorithm and standard parameters of the SoftWoRx software (Applied Precision, PA).

### Quantification of *oriC* foci

To identify fluorescent foci, stacks of images of each *Epulopiscium* sp. type B cell were analyzed using OpenCV 2.4 (opencv.org). Images were preprocessed to remove background and to improve contrast. A binary threshold isolated bright *oriC* foci from darker background. Thresholding the image results in a binary image of either true or false pertaining to above the threshold and below the threshold, respectively. Individual *oriC* was identified by clustering pixels using the DBSCAN clustering algorithm ( $\epsilon = 1$ , minPts = 2) (Martin *et al.*, 1996). The DBSCAN process considers each true pixel as a point of interest for clustering purposes based on the (x, y) coordinate of the pixel. Once clusters were identified, the center of mass for each cluster was calculated and used as a proxy for *oriC* location. Collections of *oriC* coordinates were then used to perform spatial calculations. To compute the volume of the cell, the outermost *oriCs* were used to calculate the convex hull of the cell using the QuickHull algorithm (Barber *et al.*, 1996). We then used the convex hull and the total number of *oriC* foci observed to calculate the chromosome density for the cell. The OPTICS clustering algorithm was used to classify extracellular *oriC* foci and to separate distinct *oriCs* in images with multiple cells (Ankerst *et al.*, 1999). We also used the *oriC* coordinates to visualize the two-dimensional kernel density in specific regions of the cell. For each individual *oriC*, distances to all other *oriC* foci were calculated, and the average Euclidian distance to the nearest four neighboring *oriC* foci was determined. Distance distributions were used to construct density estimation plots and to conduct statistical analyses to compare populations of cells. All scripts are available at <https://github.com/nicholasyager/epulopiscium-analysis>.

### Identification of *B. subtilis* homologs in *C. lentocellum* and *Epulopiscium* sp. type B

Genomic analyses were performed primarily using the IMG/ER database (Markowitz *et al.*, 2012). Protein sequences from *Epulopiscium* sp. type B were obtained from the draft genome sequence (Miller *et al.*, 2012). Protein sequences from *B. subtilis* were used to interrogate predicted protein sequences from *C. lentocellum* and *Epulopiscium* sp. type B. Candidate orthologs were tested using a reciprocal BLAST search to the *B. subtilis* genome. Proteins were considered orthologs if they were the top reciprocal best BLAST hit (RBBH), had query coverage of  $\geq 70\%$  and percent identity of  $\geq 30\%$ . Some proteins passed the RBBH



test but did not pass the query coverage and percent identity test. For these genes, if they exhibited synteny with *B. subtilis* and/or *C. lentocellum* homologs within an operon, they were considered a potential homolog.

## Acknowledgements

This research was supported by grants from the National Science Foundation MCB 0721583 and MCB 1244378. The authors would like to acknowledge Kendall Clements and Howard Choat for surgeonfish collection at the Lizard Island Research Station and W. Linn Montgomery, Joshua Copus and Cassie Copus for surgeonfish collection and processing at the Hawaii Institute of Marine Biology. We would also like to thank Brian Bowen at HIMB and the directors of the LIRS for providing access to lab space and resources during our stay. The authors thank Teresa Pawlowska, Wojtek Pawlowski and Choon-Lin Tiang for their assistance with and use of the deconvolution microscope. Finally, we would like to thank Marquessa Henry for her initial work on FISH using type C epulos. EAH would like to thank David Miller for providing endless expertise on working with epulos, particularly at the early stages of this project. The authors have no conflicts of interest to declare.

## Author contributions

EH and EA designed experiments and wrote the manuscript. EH and MNT conducted FISH experiments. NY and MT developed and performed computational approaches. EH, DRS and FA performed bioinformatic analyses. All reviewed the final draft of the manuscript.

## References

- Angert, E.R. (2005) Alternatives to binary fission in bacteria. *Nat Rev Microbiol* **3**: 214–224.
- Angert, E.R. (2012) DNA replication and genomic architecture of very large bacteria. *Annu Rev Microbiol* **66**: 197–212.
- Angert, E.R., and Clements, K.D. (2004) Initiation of intracellular offspring in *Epulopiscium*. *Mol Microbiol* **51**: 827–835.
- Angert, E.R., Clements, K.D., and Pace, N.R. (1993) The largest bacterium. *Nature* **362**: 239–241.
- Ankerst, M., Breunig, M.M., Kriegel, H.-P. and Sander, J. (1999) OPTICS: ordering points to identify the clustering structure. In *Proceedings of the 1999 ACM SIGMOD International Conference on Management of Data*. Philadelphia, Pennsylvania, USA: ACM, pp. 49–60.
- Barber, C., Dobkin, D., and Huhdanpaa, H. (1996) The quickhull algorithm for convex hulls. *ACM Trans on Mathematical Software* **22**: 469–483.
- Bass, J.W., Marshall, W.F., Sedat, J.W., Agard, D.A., and Cande, W.Z. (1997) Telomeres cluster de novo before the initiation of synapsis: a three-dimensional spatial analysis of telomere positions before and during meiotic prophase. *J Cell Biol* **137**: 5–18.
- Cagliero, C., Grand, R.S., Jones, M.B., Jin, D.J., and O'Sullivan, J.M. (2013) Genome conformation capture reveals that the *Escherichia coli* chromosome is organized by replication and transcription. *Nucleic Acids Res* **41**: 6058–6071.
- Chen, A.H., Afonso, B., Silver, P.A., Savage, D.F., and Isalan, M. (2012) Spatial and temporal organization of chromosome duplication and segregation in the cyanobacterium *Synechococcus elongatus* PCC 7942. *PLoS One* **7**: e47837.
- Clements, K.D., Sutton, D.C., and Choat, J.H. (1989) Occurrence and characteristics of unusual protistan symbionts from surgeonfishes (Acanthuridae) of the Great Barrier Reef, Australia. *Mar Biol* **102**: 403–412.
- David, A., Demarre, G., Muresan, L., Paly, E., Barre, F.-X., Possoz, C., and Burkholder, W.F. (2014) The two cis-acting sites, *parS1* and *oriC1*, contribute to the longitudinal organisation of *Vibrio cholerae* chromosome I. *PLoS Genet* **10**: e1004448.
- Donovan, C., Schwaiger, A., Kramer, R., and Bramkamp, M. (2010) Subcellular localization and characterization of the ParAB system from *Corynebacterium glutamicum*. *J Bacteriol* **192**: 3441–3451.
- Govindarajan, S., Nevo-Dinur, K., and Amster-Choder, O. (2012) Compartmentalization and spatiotemporal organization of macromolecules in bacteria. *FEMS Microbiol Rev* **36**: 1005–1022.
- Graumann, P.L. (2014) Chromosome architecture and segregation in prokaryotic cells. *J Mol Microbiol Biotechnol* **24**: 291–300.
- Griese, M., Lange, C., and Soppa, J. (2011) Ploidy in cyanobacteria. *FEMS Microbiol Lett* **323**: 124–131.
- Hansen, M.T. (1978) Multiplicity of genome equivalents in radiation-resistant bacterium *Micrococcus radiodurans*. *J Bacteriol* **134**: 71–75.
- Harms, A., Treuner-Lange, A., Schumacher, D., Søgaard-Andersen, L., and Burkholder, W.F. (2013) Tracking of chromosome and replisome dynamics in *Myxococcus xanthus* reveals a novel chromosome arrangement. *PLoS Genet* **9**: e1003802.
- Holmes, V.F., and Cozzarelli, N.R. (2000) Closing the ring: links between SMC proteins and chromosome partitioning, condensation, and supercoiling. *Proc Natl Acad Sci USA* **97**: 1322–1324.
- Jain, I.H., Vijayan, V., and O'Shea, E.K. (2012) Spatial ordering of chromosomes enhances the fidelity of chromosome partitioning in cyanobacteria. *Proc Natl Acad Sci USA* **109**: 13638–13643.
- Jakimowicz, D., and van Wezel, G.P. (2012) Cell division and DNA segregation in *Streptomyces*: how to build a septum in the middle of nowhere? *Mol Microbiol* **85**: 393–404.
- Jensen, R.B., and Shapiro, L. (1999) The *Caulobacter crescentus* *smc* gene is required for cell cycle progression and chromosome segregation. *Proc Natl Acad Sci USA* **96**: 10661–10666.
- Jose Lopez-Sanchez, M., Neef, A., Patino-Navarrete, R., Navarro, L., Jimenez, R., Latorre, A., and Moya, A. (2008) *Blattabacteria*, the endosymbionts of cockroaches,



- have small genome sizes and high genome copy numbers. *Environ Microbiol* **10**: 3417–3422.
- Jun, S., and Mulder, B. (2006) Entropy-driven spatial organization of highly confined polymers: lessons for the bacterial chromosome. *Proc Natl Acad Sci USA* **103**: 12388–12393.
- Jun, S., and Wright, A. (2010) Entropy as the driver of chromosome segregation. *Nat Rev Microbiol* **8**: 600–607.
- Laloux, G., and Jacobs-Wagner, C. (2014) How do bacteria localize proteins to the cell pole? *J Cell Sci* **127**: 11–19.
- Le, T.B., and Laub, M.T. (2014) New approaches to understanding the spatial organization of bacterial genomes. *Curr Opin Microbiol* **22**: 15–21.
- Le, T.B., and Laub, M.T. (2016) Transcription rate and transcript length drive formation of chromosomal interaction domain boundaries. *EMBO J* **35**: 1582–1595.
- Le, T.B., Imakaev, M.V., Mirny, L.A., and Laub, M.T. (2013) High-resolution mapping of the spatial organization of a bacterial chromosome. *Science* **342**: 731–734.
- Lenarcic, R., Halbedel, S., Visser, L., Shaw, M., Wu, L.J., Errington, J., *et al.* (2009) Localisation of DivIVA by targeting to negatively curved membranes. *EMBO J* **28**: 2272–2282.
- Maloney, E., Madiraju, M., and Rajagopalan, M. (2009) Overproduction and localization of *Mycobacterium tuberculosis* ParA and ParB proteins. *Tuberculosis (Edinb)* **89**(Suppl. 1): S65–S69.
- Marbouty, M., Le Gall, A., Cattoni, D.I., Cournac, A., Koh, A., Fiche, J.-B., *et al.* (2015) Condensin- and replication-mediated bacterial chromosome folding and origin condensation revealed by Hi-C and super-resolution imaging. *Mol Cell* **59**: 588–602.
- Markowitz, V.M., Chen, I.-M.A., Palaniappan, K., Chu, K., Szeto, E., Grechkin, Y., *et al.* (2012) IMG: the Integrated Microbial Genomes database and comparative analysis system. *Nucleic Acids Res* **40**: D115–D122.
- Martin, E., Kriegel, H.-P., Sander, J. and Xu, X. (1996) A density-based algorithm for discovering clusters in large spatial databases with noise. In *Proceedings of the Second International Conference on Knowledge Discovery and Data Mining (KDD-96)*. Simoudis, E., Han, J., and Fayyad, U.M. (eds). Palo, Alto, CA: AAAI Press, pp. 226–231.
- Mendell, J.E., Clements, K.D., Choat, J.H., and Angert, E.R. (2008) Extreme polyploidy in a large bacterium. *Proc Natl Acad Sci USA* **105**: 6730–6734.
- Michelsen, O., Hansen, F.G., Albrechtsen, B., and Jensen, P.R. (2010) The MG1363 and IL1403 laboratory strains of *Lactococcus lactis* and several dairy strains are diploid. *J Bacteriol* **192**: 1058–1065.
- Miller, D.A., Choat, J.H., Clements, K.D., and Angert, E.R. (2011) The *spolIE* homolog of *Epulopiscium* sp. type B is expressed early in intracellular offspring development. *J Bacteriol* **193**: 2642–2646.
- Miller, D.A., Suen, G., Clements, K.D., and Angert, E.R. (2012) The genomic basis for the evolution of a novel form of cellular reproduction in the bacterium *Epulopiscium*. *BMC Genomics* **13**: 265.
- Minton, K.W. (1994) DNA-repair in the extremely radioreistant bacterium *Deinococcus radiodurans*. *Mol Microbiol* **13**: 9–15.
- Mohl, D.A., and Gober, J.W. (1997) Cell cycle-dependent polar localization of chromosome partitioning proteins in *Caulobacter crescentus*. *Cell* **88**: 675–684.
- Nielsen, H.J., Ottesen, J.R., Youngren, B., Austin, S.J., and Hansen, F.G. (2006) The *Escherichia coli* chromosome is organized with the left and right chromosome arms in separate cell halves. *Mol Microbiol* **62**: 331–338.
- Niki, H., Yamaichi, Y., and Hiraga, S. (2000) Dynamic organization of chromosomal DNA in *Escherichia coli*. *Genes Dev* **14**: 212–223.
- Ohtani, N., Tomita, M., and Itaya, M. (2010) An extreme thermophile, *Thermus thermophilus*, is a polyploid bacterium. *J Bacteriol* **192**: 5499–5505.
- Pecoraro, V., Zerulla, K., Lange, C., Soppa, J., and Aziz, S. (2011) Quantification of ploidy in Proteobacteria revealed the existence of monoploid, (mero-)oligoploid and polyploid species. *PLoS One* **6**: e16392.
- Ramamurthi, K.S. (2010) Protein localization by recognition of membrane curvature. *Curr Opin Microbiol* **13**: 753–757.
- Ramamurthi, K.S., and Losick, R. (2009) Negative membrane curvature as a cue for subcellular localization of a bacterial protein. *Proc Natl Acad Sci USA* **106**: 13541–13545.
- Reyes-Lamothe, R., Nicolas, E., and Sherratt, D.J. (2012) Chromosome replication and segregation in bacteria. *Annu Rev Genet* **46**: 121–143.
- Robinow, C., and Angert, E.R. (1998) Nucleoids and coated vesicles of *Epulopiscium* spp. *Arch Microbiol* **170**: 227–235.
- Roggiani, M., and Goulian, M. (2015) Chromosome-membrane interactions in bacteria. *Annu Rev Genet* **49**: 115–129.
- Schneider, D., Fuhrmann, E., Scholz, I., Hess, W.R., and Graumann, P.L. (2007) Fluorescence staining of live cyanobacterial cells suggest non-stringent chromosome segregation and absence of a connection between cytoplasmic and thylakoid membranes. *BMC Cell Biol* **8**: 39.
- Schulz, H.N., Brinkhoff, T., Ferdelman, T.G., Marine, M.H., Teske, A., and Jorgensen, B.B. (1999) Dense populations of a giant sulfur bacterium in Namibian shelf sediments. *Science* **284**: 493–495.
- Teleman, A.A., Graumann, P.L., Lin, D.C., Grossman, A.D., and Losick, R. (1998) Chromosome arrangement within a bacterium. *Curr Biol* **8**: 1102–1109.
- Toro, E., and Shapiro, L. (2010) Bacterial chromosome organization and segregation. *Cold Spring Harb Perspect Biol* **2**: a000349.
- Tzeng, L., and Singer, M. (2005) DNA replication during sporulation in *Myxococcus xanthus* fruiting bodies. *Proc Natl Acad Sci USA* **102**: 14428–14433.
- Vallet-Gely, I., and Boccard, F. (2013) Chromosomal organization and segregation in *Pseudomonas aeruginosa*. *PLoS Genet* **9**: e1003492.
- Viollier, P.H., Thanbichler, M., McGrath, P.T., West, L., Meewan, M., McAdams, H.H., and Shapiro, L. (2004) Rapid and sequential movement of individual chromosomal loci to specific subcellular locations during bacterial DNA replication. *Proc Natl Acad Sci USA* **101**: 9257–9262.

- Wang, X., and Rudner, D.Z. (2014) Spatial organization of bacterial chromosomes. *Curr Opin Microbiol* **22**: 66–72.
- Wang, X., Liu, X., Possoz, C., and Sherratt, D.J. (2006) The two *Escherichia coli* chromosome arms locate to separate cell halves. *Genes Dev* **20**: 1727–1731.
- Wang, X., Montero Llopis, P., and Rudner, D.Z. (2014) *Bacillus subtilis* chromosome organization oscillates between two distinct patterns. *Proc Natl Acad Sci USA* **111**: 12877–12882.
- Wang, X.D., Llopis, P.M., and Rudner, D.Z. (2013) Organization and segregation of bacterial chromosomes. *Nat Rev Genet* **14**: 191–203.
- Ward, R.J., Clements, K.D., Choat, J.H., and Angert, E.R. (2009) Cytology of terminally differentiated *Epulopiscium* mother cells. *DNA Cell Biol* **28**: 57–64.
- Webb, C.D., Teleman, A., Gordon, S., Straight, A., Belmont, A., Lin, D.C., et al. (1997) Bipolar localization of the replication origin regions of chromosomes in vegetative and sporulating cells of *B. subtilis*. *Cell* **88**: 667–674.
- Young, K.D. (2006) The selective value of bacterial shape. *Microbiol Mol Biol Rev* **70**: 660–703.
- Youngren, B., Nielsen, H.J., Jun, S., and Austin, S. (2014) The multifork *Escherichia coli* chromosome is a self-duplicating and self-segregating thermodynamic ring polymer. *Genes Dev* **28**: 71–84.

### Supporting information

Additional supporting information may be found in the online version of this article at the publisher's web-site.